Conceptual Design of a Variable Geometry, Axial Flow Turbocharger Turbine

Author, co-author (Do NOT enter this information. It will be pulled from participant tab in MyTechZone)

Affiliation (Do NOT enter this information. It will be pulled from participant tab in MyTechZone)

Abstract

The modern automotive industry is under strict regulations to reduce emissions to comply with the Kyoto Protocol, a universally acknowledged treaty aiming at reducing exhaust gas emissions. In order to achieve the required future emission reduction targets, further developments on gasoline engines are required. One of the main methods to achieve this goal is the application of engine downsizing. Turbocharging is a cost-effective method of downsizing an engine whilst reducing exhaust gas emissions, reducing fuel consumption and maintaining prior performance outputs. For these reasons, the turbocharging is becoming the most widely adopted technology in the automotive markets. In 2012, 32% of passenger and commercial vehicles sold had a turbocharger installed, and is predicted to be 40% of 2017 [1]. Even if the engine turbocharging is a widespread technology, there are still drawbacks present in current turbocharging systems. The main problem is overcoming the issue of turbo-lag, which is the poor initial response of the turbocharger to the driver commands due to its inertia. Indeed, the system turbine plus compressor is characterized by an own rotational inertia, therefore, the turbocharger will take a certain time to accelerate and produce the desired boost when a higher amount of exhaust gas is sent to the system. In this work, an innovative solution to the turbo-lag phenomenon will be analyzed: a vaneless stator-axial flow turbine. The proposed turbine configuration would improve the transient response of the system since the axial turbine has intrinsically a lower inertia than the radial turbine as stated by the research works of Ford first [2] and Honeywell after [3]. The whole design process is presented in this paper and particular relevance has been given to the thermo-fluid-dynamic aspect of the machine. Several CFD investigations have been carried out in order to deeply understand the new turbine behavior and, thanks to a 1D model of the target engine, it has been possible to validate the new design simulating the performance of the system engine + turbocharger.

Introduction

In 2014 a patent was published that describes an innovative technology: the Dual-Boost turbocharger. One of the many interesting features of this unconventional turbocharger, conceived to be matched with a gasoline engine, is the replacement of the common radial turbine with an axial one. The axial turbine has intrinsically a lower inertia than the radial turbine that would deliver 25% improvement in time to torque. Furthermore, the turbine will work at very variable blade speed ratio (U/Co). Turbine efficiency at such conditions is normally poor making it difficult to extract energy and accelerate quickly. Improving the turbine efficiency at low U/Co conditions would produce benefits in both transient and steady state performance of the turbocharger and engine. The axial turbine has higher efficiency at low U/Co than the radial one [3]. The Honeywell idea could be considered the starting point of this project that aims to replace the actual turbine of an existing Garrett turbocharger. The new turbine design will substantially differ from the most typical structure of axial turbines used for power generation or aeronautic propulsion. In fact, as in the Dual Boost turbocharger, the axial flow turbine will be equipped with a vaneless stator. The exhaust gases coming from cylinders, will be firstly accelerated in a volute, rotated 90 degrees from radial to the axial direction and then will flow through a variable area nozzle and finally provide work to the rotor. While the volute will not present any substantial difference compared to a usual radial turbine volute, the device that will perform the 90° turning of the gas is a unique aspect of the project; it will be hereafter called “nozzle”. The nozzle of the new axial turbine will be a vaneless truncated-cone shaped channel. The design of the blading row will be performed trying to achieve high efficiency in a wide range of operating conditions and to deliver a suitable amount of power. Another design criterion followed during the whole project is to not exceed the size of the original turbine.
As already explained, the new axial design will replace an existing radial turbine, this means that the new machine should ensure almost the same engine performance as the original one in terms of power and torque. For this reason, the final section of this papers evaluates the turbocharger – engine matching in order to estimate the benefits that are aspect from the novel turbine concept.

Methodology

The design process of a turbomachine requires assignment of a set of input parameters and, in the case of a turbocharging turbine, such parameters are the thermo-fluid-dynamic conditions of exhaust gases into the exhaust piping system of the engine. The target engine selected for the application is a medium-small size gasoline engine: the 1,6 liter Ford EcoBoost. Due to the lack of data, it has been decided to build a 1D model of a real engine. The data provided by the model substitutes the unknown parameters necessary to perform the design phase. The turbocharger that boosts this Ford engine is a BorgWarner one, therefore, since the objective is to modify a Garrett turbocharger, during the development of the 1D model, a new (Garrett) turbo has been matched with the engine.

Engine 1D modelling

The engine model was built using the software Ricardo Wave® to reproduce the most common configuration of actual engines of the 1.6L EcoBoost category. The development of the model involved a massive calibration and validation activity. The provided engine data are the power and torque curves and the combustion trends at full load conditions. So, the model calibration activity involved the research of the suitable values for the other parameters in order to match the real engine behavior. In particular, the objective was to reproduce the same power and torque curves of the real engine.

Figure 1 shows the 1D engine model and it is possible to identify the main parts of the engine.

Furthermore, the development of this model involved the selection of a new turbocharger within the Garrett catalogue, since the activity aims to replace the turbine of a Garrett turbocharger. The selection has been carried out following the usual Garrett procedure that suggested the GT1548 as the best suiting turbo for the target 1.6 liter EcoBoost. Regarding to the waste-gate actuation system, it has been simulated employing a PID controller (see Figure 1). The system checks the pressure value at the compressor outlet port adjusting the exhaust gas quantity that flows into the turbine, like a real waste-gate valve. The calibration activity allowed the model, coupled with the GT1548 turbo, to accurately simulate the performance of the real EcoBoost; Figure 2 and Figure 3 shows the model results comparing calculated and real performance curves: the simulated values are within a ±2% tolerance.

Table 1. Principal engine parameters at different rpm and 100% of load

Engine Speed (maximum load)	[rpm]	6000	5000	4000	3000	2000
Total Pressure Rotor Inlet	[bar]	2.27	2.38	1.97	1.67	1.32
Tot Temperature Rotor Inlet	[K]	1050	1090	1066	1040	1039
Specific Heat Ratio	[-]	1.33	1.33	1.33	1.33	1.33
Specific Heat	[kJ/kg/K]	1.15	1.15	1.15	1.15	1.15
Gas Constant	[J/kg/K]	285	285	285	285	285
Rotational Speed	[krpm]	137	146	132	115	87
Static Pressure Rotor Outlet	[bar]	1.37	1.46	1.28	1.17	1.08
Pressure Ratio	[-]	1.65	1.62	1.53	1.43	1.23
Mach Number Rotor Outlet	[-]	0.3	0.3	0.3	0.3	0.3
Total Pressure Rotor Outlet	[bar]	1.46	1.55	1.36	1.24	1.14
Mass Flow Rate	[kg/s]	0.11	0.11	0.09	0.07	0.04
Tot. Temp. Rotor Outlet	[K]	941	981	973	966	1002
Static Temp. Rotor Outlet	[K]	927	966	958	952	987
Static Density Rotor Outlet	[kg/m^3]	0.52	0.53	0.47	0.43	0.38
Total to Total Enthalpy Drop	[kJ/kg]	125	125	107	84	42

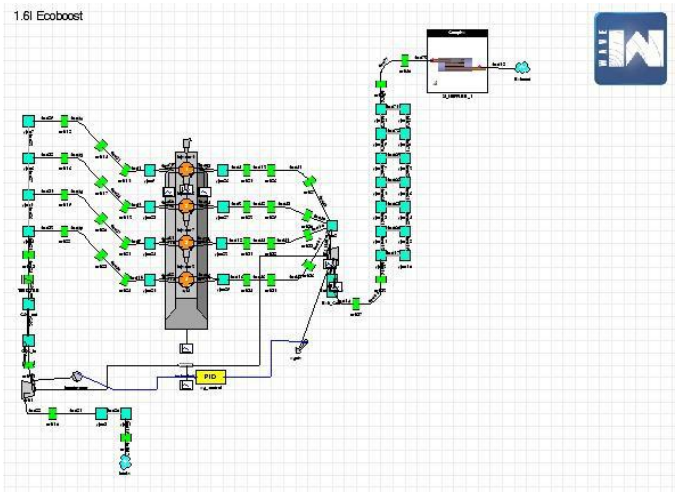

Figure 1. 1D model of the EcoBoost engine

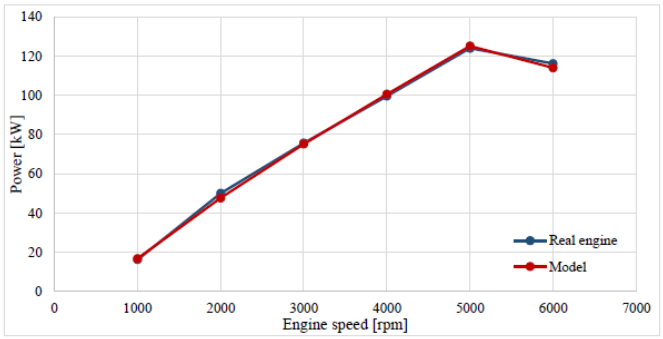

Figure 2. Calculated power curve vs. real engine power curve

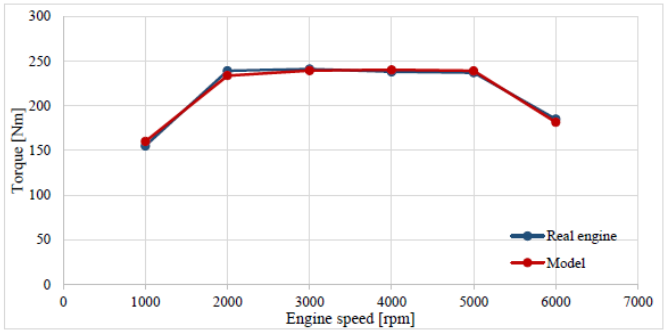

Figure 3. Calculated torque curve vs. real engine torque curve

The results of the calibrated engine model represent the boundary conditions for the turbine design process. Table 1 shows that the thermo-fluid-dynamic condition of the exhaust gas are strongly variable with the engine speed. Thus, the first step of the design process will involve the selection of a single engine operating condition as turbine design point.

Specific Speed and Diameter Analysis

In general, an axial machine is suitable to work higher flow and to rotate at higher speeds, while the radial turbine is able to process in a single stage a greater enthalpy drop. Before the design process, it is reasonable a preliminary analysis of the specific speed at the different operation points obtained from the engine simulation to justify the choice of the axial turbine, or at least to check if an automotive turbocharger is a reasonable application for an axial turbine. Therefore, the specific speed of a machinery defines its suitability for a specific application [4]. The specific speed is defined as follows:

$$Ns = \frac{\omega\sqrt{\frac{\dot{m}}{\rho}}}{\Delta h_{t,id}{}^{3/4}} \quad (1)$$

The specific diameter is another dimensionless parameter that allows the designer to choose the most suitable type of machinery for the current application as well as the specific speed. It is calculated as follows:

$$Ds = \frac{Dm\ \Delta h_{ts,id}{}^{1/4}}{\sqrt{\frac{\dot{m}}{\rho}}} \quad (2)$$

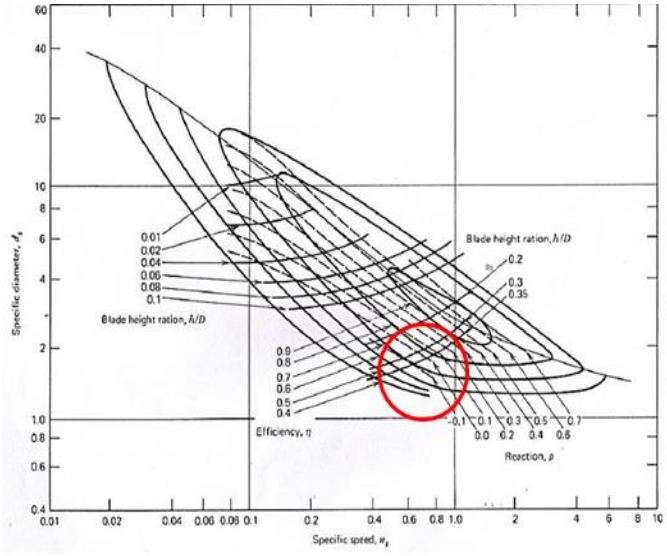

Figure 4. Balje diagram

Both *Ns* and *Ds* have been calculated for different engine operating conditions at full load and 75% load. Therefore, the values of *Ns* and *Ds* calculated for each considered operating condition define an area on the Balje diagram, see Figure 4. The Balje diagram gives an expectation of the turbine efficiency as a function of *Ns* and *Ds* and the calculated values of *Ns* and *Ds* fall within a good efficiency zone (red circle, 70-80%) for a turbocharger turbine. This means that the idea of replacing the radial turbine with an axial one is reasonable for this application [5].

Design Point Selection

The design point of a turbomachine is the operation condition in which it gives the best performance, variables between power, efficiency and others depending on the specific use, and thus the point where it matches the project objectives. In the case of a turbocharger that must be coupled to a thermal machine, the choice could be very difficult because the ICE is characterized by a very wide operating range. The philosophy that has been decided to follow in this study is exactly this: size the turbine for the conditions of flow, pressure and temperature that occur at engine speed corresponding to maximum torque at 75% of load. It is clear that this would involve a satisfying capacity of the turbo-engine system to deliver a high amount of torque at high rpm; but, at lower rpm, the exhaust gas flow rate is smaller and less energized, so that it will not be able to move the turbine wheel efficiently and obtain a suitable turbocharging level. Anyway, this choice has been done considering the possibility of a variable geometry mechanism, designed to improve the response of the turbine (and thus of the engine) in the conditions of lower flow rates and pressures of the exhausts.

Table 2 shows the output of the 1D engine model at the selected design point.

Table 2. Design point information

Design condition: Maximum torque at 75% load		
Engine speed	[rpm]	5000
Mass flow	[kg/s]	0.113
Inlet pressure	[bar]	2.3536
Outlet pressure	[bar]	1.4575
Pressure ratio	[-]	1.6148
Turbine Speed	[rpm]	145669
Inlet temperature	[K]	1097.34
Outlet temperature	[K]	1042.24
Produced power	[W]	8164.16

Rotor preliminary design

This step of the design aims to generate the geometry of the blade row starting with a certain number of fixed parameters and calculating the dimension of each vector part of triangles of velocity. In the initial phase of a turbine development study some of the principal design parameters have to be assumed or imposed but then they will be optimized to match the goal of the project.

Before using a commercial software to perform the preliminary design phase of the turbine rotor, another in-house built code has been used. The reasons for that are two. Firstly, it could be useful to approach to the commercial software knowing the precise value to impose to each parameter. Secondly, as described before, the new turbine will be a vane-less stator axial turbine, which means that the acceleration of the fluid (i.e. the conversion of the static enthalpy in kinetic energy) is provided by the combined action of the volute and of a unique nozzle. This is an innovative configuration and it is not contemplated in the commercial preliminary design software.

Axturb

Axturb is the name of the code used in that phase that could be called pre-preliminary design phase. That code, developed internally at DII (Department of Industrial Engineering) of the University "Federico II" of Naples, is not only able to determine the triangle of velocity starting from a certain number of input data, but it gives the possibility to examine different off-design cases. In fact, it is possible to import a set of values for each design parameter and then the code identifies the most efficient combination without discarding other solutions. Furthermore, Axturb includes a sophisticated loss prediction model, the Craig and Cox model [6]. Axturb also allows to calculate a stator-less turbine configuration.

AxStream

One of the reasons why AxStream was chosen as a tool for the preliminary design was the possibility to set the calculations with updated loss models and currently available in the literature. Indeed, for primary profile losses and secondary losses the Kacker-Okapuu model has been employed while for calculating the deviation angle, the relation of Ainley and Mathieson. The input data to be set to start the research of the possible solutions by AxStream were derived partly from the calculations performed with Axturb, and partly derived from simulations with Ricardo WAVE and others are values recommended by the guide of the software itself. AxStream generates

a domain of solutions and the selected solution is a compromise among total-to-static efficiency, total-to total efficiency and dimension of the rotor. In fact, it is a common practice to use a rotor wheel with a diameter comparable to the diameter of the compressor wheel (that is, for the GT1548 compressor, 48.6 mm).

The selected AxStream solution presents the following rotor dimension: maximum axial length (at the rotor hub) of 14.2 mm, average blade height of 10.5 mm and 48.7 mm for the tip diameter.

The optimum number of rotor blades calculated in the preliminary phase is 12. Anyway, a dedicated CFD analysis has been carried out to find the final number of blades. In fact, the more the number of blades increases, the more the fluid is well-guided throughout each rotor passage but the more the friction losses between fluid and blade and the weight of the rotor (and its inertia) increase. So, a trade-off must be found between weight and efficiency. The CFD investigation will not be presented in this paper for brevity; it involved the simulation of different rotor configurations with a different number of blades. It was found that tin a he best compromise is the rotor with 16 blades.

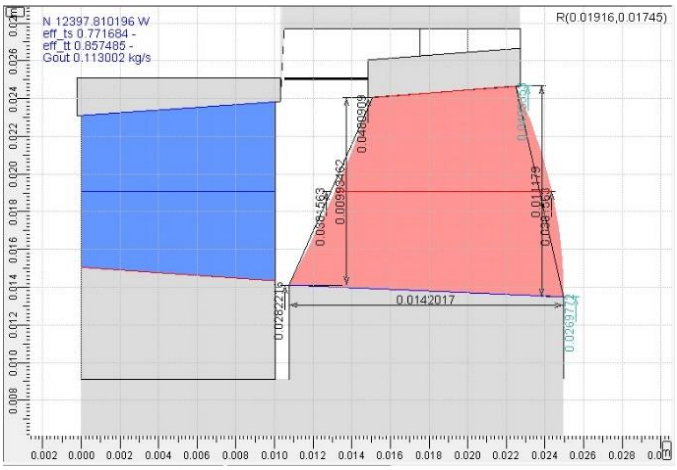

Figure 5. Annulus of the machine with some dimensions, [7]

Furthermore, even if the software produces a classic turbine configuration (stator blade row + rotor blade row) as shown in Figure 5, the final design consists in a vane-less stator, as specified. The design of the other two components of the turbine has been carried out keeping unvaried the flow condition at the inlet section of the rotor calculated by AxStream.

Volute and nozzle preliminary design

Nozzle design

The preliminary design of the nozzle has been done using a one-dimensional approach. In a radial turbine, the bladed nozzle accelerates the fluid and impresses the right direction to it to reduce the incidence losses at the rotor inlet; in this case, the nozzle must turn 90° the fluid that comes from the volute circumferentially and must enter the rotor axially. Therefore, it is expected that the inlet section and the outlet section of the nozzle will be rotated of 90 degrees one other. The nozzle of this new axial turbine will be a vane-less nozzle, that will make it less expensive and simpler than a bladed one. It was also decided, for simplicity, to adopt a constant cross-sectional area nozzle. Thus, this configuration does not accelerate the radial component of the flow.

Neglecting every loss into the nozzle and indicating with the subscript "1" the parameters relative to the nozzle inlet section and with the subscript "2" the ones relative to the nozzle outlet section, the radial velocity C_{1r} will be only turned in the axial direction by the nozzle but its value will remain constant being the cross section of the nozzle constant. Therefore, C_{1r} must be equal to C_{2x}, the axial component of the velocity at rotor inlet. According to the conservation of angular momentum, $C_{1\theta}$ must respect the following relationship:

$$C_{1\theta}r_1 = C_{2\theta}r_2 \quad (3)$$

It is now clear that the dimensions of the nozzle must respect the following relationships:

$$C_{1r} = C_{2x}; \quad (4) \quad A_1 = A_2 \rightarrow 2\pi r_1 b_1 = 2\pi r_2 b_2 \quad (5)$$

$$C_{1\theta}r_1 = C_{2\theta}r_2 \quad (6)$$

The dimension of the rotor imposes the value of r_2 that must be equal to the mean radius of the rotor and b_2 that must be equal to the height of the blade. The value of r_1 depends on the value of $C_{1\theta}$ achievable by the volute, for this reason, in this phase a reasonable value of r_1 is fixed and a value of $C_{1\theta}$ is calculated. Then, if the volute will not be able to achieve the desired value of $C_{1\theta}$, r_1 will be changed iteratively. Finally, it should be fixed a value of the axial length of the nozzle, this value must not be too high because it effects the total dimension of the turbine side, 10 mm was judged a suitable value.

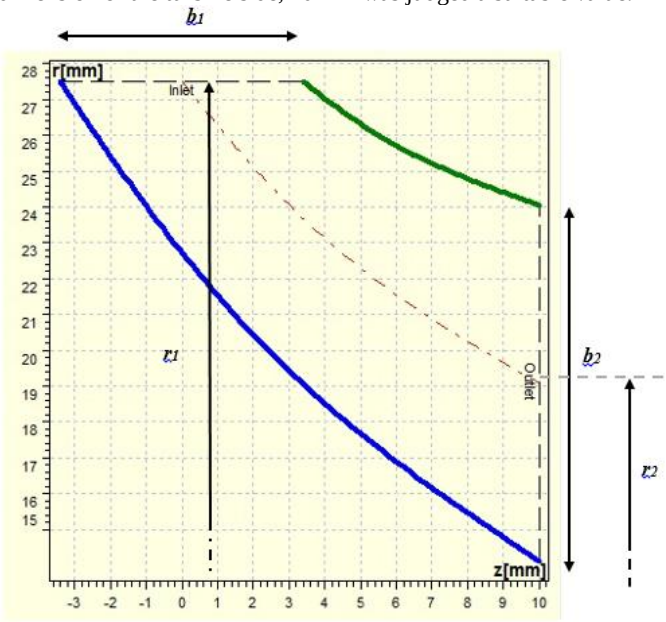

Figure 6. 2D view of the nozzle

Volute design

The volute has been designed in a preliminary phase in a similar manner to the one-dimensional flow analysis of the nozzle. The objective of the design is to realize a geometry that determines the desired flow angle and velocity at volute exit. In fact, the flow angle and velocity should not depart from the values calculated by AxStream to achieve the predicted turbine performance. The volute can be designed using incompressible flow theory with constant angular momentum (and hence uniform pressure) [8].

From Figure 7:

$$rC_\theta = constant = K \quad (7)$$

For incompressible flow, the mass flow rate at an azimuth angle ψ is:

$$\dot{m}_\psi = \rho A_\psi C_{\theta\psi} \quad (8)$$

Where ψ is measured counterclockwise from the volute inlet section (as shown in Figure 7).

For uniform mass flow distribution:

$$\dot{m}_\psi = \dot{m}\frac{\psi}{2\pi} \quad (9)$$

where $\dot{m}$ = total mass flow rate entering the volute. Hence

$$A_\psi = \frac{\dot{m}}{\rho C_{\theta\psi}}\frac{\psi}{2\pi} \rightarrow A_\psi = \frac{\dot{m}}{\rho}\frac{\psi}{2\pi}\frac{r_\psi}{K} \quad (10)$$

that is the cross-sectional area of the volute reduces when the azimuth decreases from a value of 2π to 0. The mean radius will vary as the volute curves in round the circumference and the area is often reduced linearly with the azimuth angle.

$$cot\alpha_1 = \frac{C_{r\psi}}{C_{\theta\psi}} \quad (11)$$

If the parameters referred to the inlet section of the volute are labelled with the subscript "0", it is possible to write the following equations:

being $r_0 C_{0\theta} = r_1 C_{1\theta}$ and $\dot{m} = \rho_0 A_0 C_{0\theta} = \rho_1 2\pi r_1 b_1 C_{1r}$, for incompressible flow $cot\alpha_1 = \frac{A_0}{r_0 2\pi b_1}$.

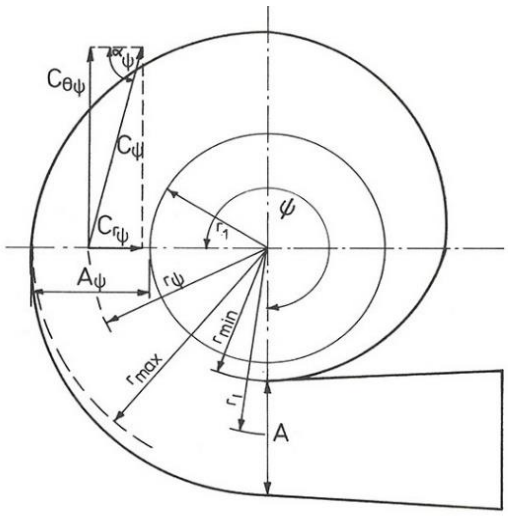

Figure 7. Velocity components of the flow within the volute, [8]

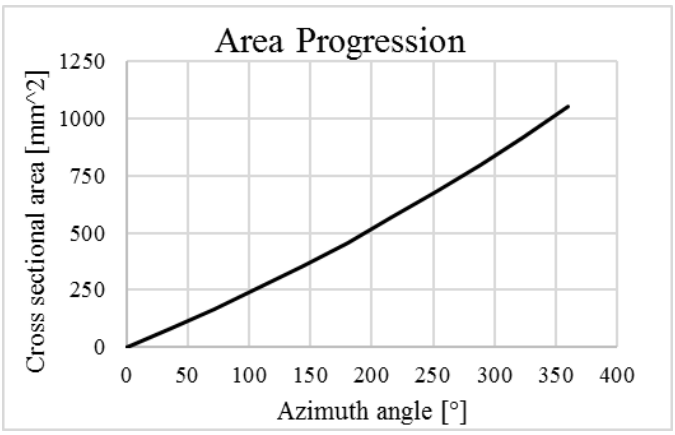

Figure 8. Volute cross sectional area progression

The previous relationships have been memorized in a spreadsheet able to calculate for each value of the azimuth angle the cross-sectional area of the volute. The resulting progression of the cross-sectional area can is illustrated in Figure 8.

Rotor 3D design and meshing

The design of the rotor was an iterative process that involved CFD simulations, results analysis, comparison with previous simulation data and geometry improvement. At first, a blade has been built up using the preliminary geometry calculated with AxStream and used as starting point for the loop calculation.

Blade 3D design

To design a 3D model of blades it has been used BladeGen, a tool of the Ansys package. The first blade profile has been developed with the blade angles and the annulus size (see Figure 5) given by Axstream, then BladeGen has been used to iteratively upgrade the blade geometry according to the results of the several CFD simulations.

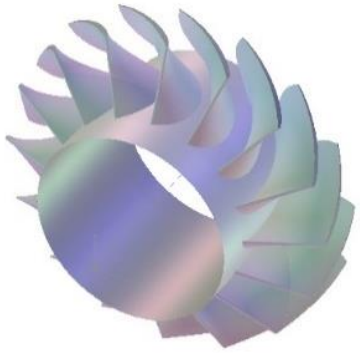

Figure 9. 3D view of the rotor

Rotor meshing

The number of elements of a mesh strongly effects the accuracy of the solution but, at the same time, it effects the computational cost of the simulation. It is important to choose the number of cells looking also at the time required to simulating. Later, in this paper, it is presented an investigation that allowed to identify the most suitable number of mesh cells for this application. From now on every described mesh generation process will follow the indications of that investigation. To generate a mesh of the rotor fluid domain it was used another software of the Ansys package: TurboGrid.

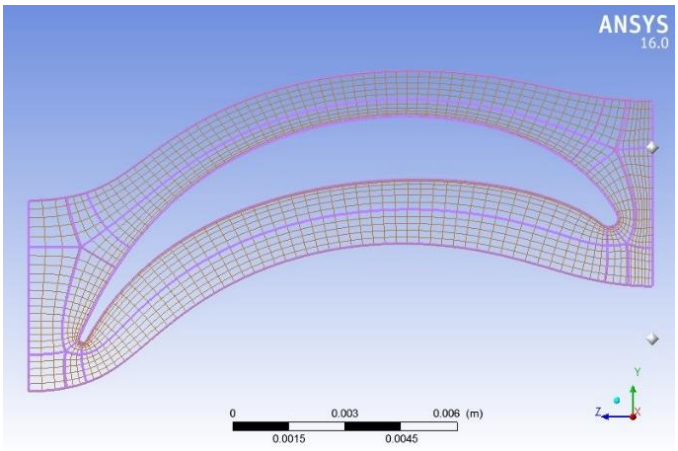

Figure 10. Topology of a mesh layer

The topology in Figure 10 already suggests the characteristics of the grid, it will be a multiblock hexahedral mesh. According to the investigation presented later, the number of cells selected was 80k with 30 rows of elements in spanwise direction. TurboGrid works on a single fluid passage, as can be observed in Figure 11, so the number of elements reported are related to just one of the 16 passages, totaling more than 1.3 million of cells for the entire rotor.

Furthermore, an increase in density of the mesh in the boundary layer of the blade has been imposed to capture accurately the flow behavior in the near wall area. Considering the small size of the fluid passage that is only one-sixteenth of the whole rotor and the total number of elements, this mesh can be considered dense.

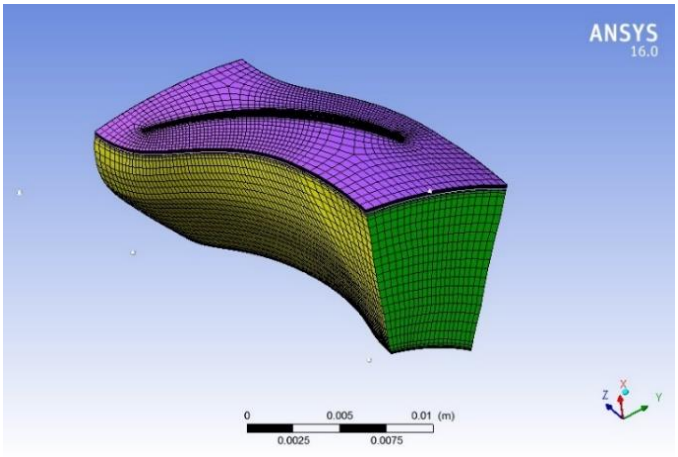

Figure 11. 3D view of single rotor channel mesh

Volute and nozzle 3D design and meshing

As seen for the rotor blading in the previous paragraph, now it will be presented the 3D design and meshing process of the fixed part of the turbine. The software employed in this phase of the project is CFturbo 10.

Volute 3D design

Firstly, the required thermodynamic conditions have been specified at the inlet and outlet of the volute; this allows the software to predict the pressure, temperature and velocity (intensity and direction) of the fluid at the volute outlet. This preliminary calculation can be useful as guide in the following phase.

The cross-sectional area progression calculated before and shown in Figure 8, was imported into CFturbo that develops the 3D geometry. Furthermore, the flow in the volute is very complicated due to the high degree of turning and the presence of a recirculation region around the tongue [9]. If the starting geometry is a sharp connection; it can be modified through changing the tongue leading by increasing θt (see Figure 12) and adding a rounded region with Rt as its characteristic [10].

By increasing the tongue angle, the total pressure loss increases. Nevertheless, the shape of the tongue should not be too sharp; otherwise, the software will not be able to create the surfaces that form that area of the volute. So, the selected shape of the tongue is a compromise between a reduction of pressure loss and the capability of the software in creating the 3D model. A fluid domain of the 3D volute can be also extracted ready to be mesched and then analysed through a CFD simulation.

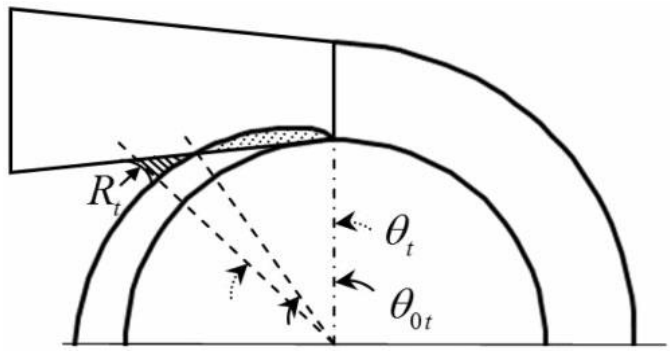

Figure 12. Volute tongue geometry, [9]

Nozzle 3D design

The process followed for modelling the nozzle was easier than the previous one; in fact, it was enough to impose the right dimensions calculated in the preliminary design phase. The unique particularity is the shaping of the hub and shroud surface of the nozzle. CFturbo generates the profile of the hub and of the shroud of the nozzle as two Bezier curves, so it is possible to stretch the control points of the curves to obtain the desired shape, a shape, in this case, that keeps constant the meridional flow velocity (constant cross section area). Figure 13 shows the fluid domain of nozzle and volute tighter in the same configuration they will be analyzed.

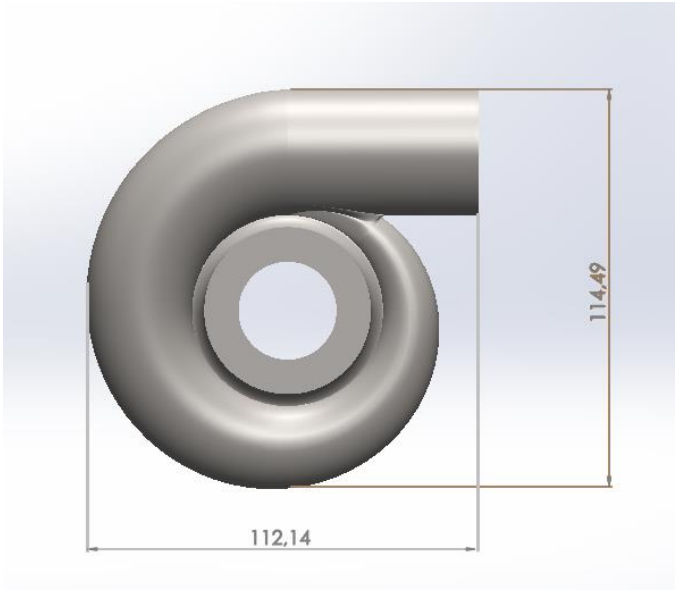

Figure 13. External dimension of the machine fixed part

Volute and Nozzle meshing

The geometry showed in Figure 13 has been meshed using another software available in Ansys suite, ICEM. Figure 14 shows the final mesh of the volute and the nozzle: it is a hybrid mesh and consists for the most part of hexahedral elements while, in a restricted region of the grid, the elements are tetrahedral; a high level of smoothing and a slow transition make the quality of this mesh noticeable; the minimum dimension of the mesh elements is 0.0001 m. The number of mesh elements is 500k as indicated by the sensibility analysis presented later that suggests 500k elements. Moreover, an inflation layer meshing is used to accurately capture the boundary layer region for any wall-bounded turbulent flows. This will provide a more accurate resolution of the boundary layer.

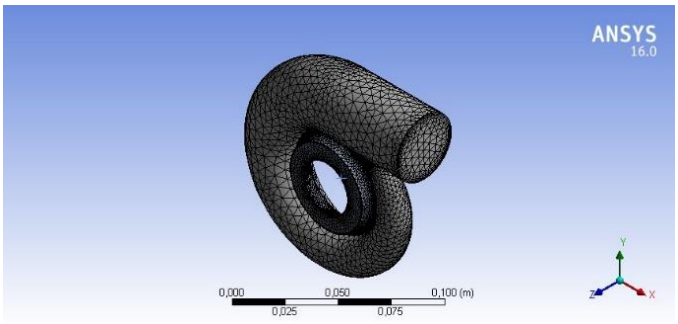

Figure 14. ICEM volute and nozzle mesh

CFD analysis of the fixed part of the turbine

The meshes of the volute and of the nozzle have been imported into Fluent to set up a CFD simulation. The setting of the simulation was very simple due to the simple geometry, the problem is stationary and each element is fixed. The definition of the boundary condition was simple as well, because there are just one inlet surface and one outlet surface, obviously, it was necessary to define an interface between volute and nozzle. The fluid chosen was air and the model of fluid was "ideal gas" but the constant value of the specific heat it has been replaced by a c_p variable with the temperature according to a 8th degree polynomial. The turbulence model chosen for this simulation was the "Reynold's Stress Model". Finally, total pressure and total temperature have been imposed as inlet boundary condition and the mass flow rate as outlet boundary condition. Some of the results of the CFD analysis are now presented.

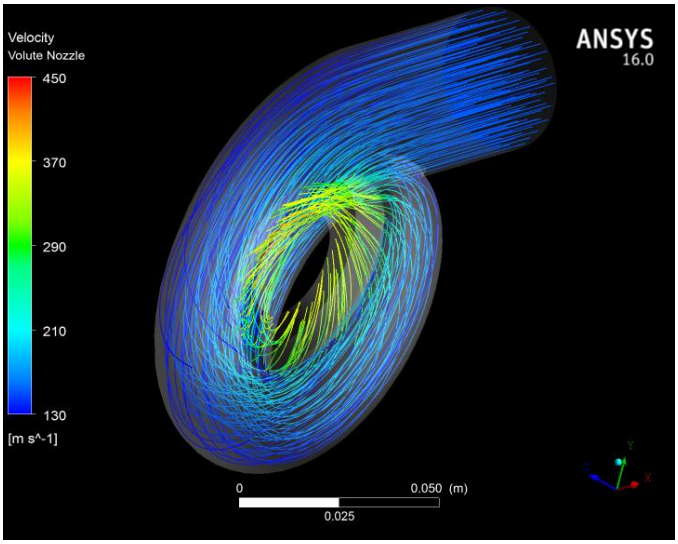

Figure 15. Streamlines identify the path of the fluid within the fixed part of the turbine

Figure 15 displays the streamlines and it is possible not only to identify the path of the fluid through the volute and the nozzle, but also the acceleration that the gas undergoes. The first check to be made is on the fluid conditions at the nozzle outlet surface; Figure 16, 17 and 18 show the contours of velocity components and angle. The most interesting aspect, except the values of the velocity, is the non-uniformity of the plotted quantities. This behavior was expected because the shape of the volute is not axisymmetric due to the presence of the tongue that, as explained, causes a distortion of the flow. The code also calculated the standard deviation of both circumferential and axial components of velocity on the outlet section of the nozzle to estimate the scattering from their area-weighted average values. The standard deviation is 65.7 m/s for the circumferential component and 59.9 m/s for the axial one. That demonstrates a not negligible non-uniformity of the flow.

Anyway, leaving aside the very low value of the velocity near walls due to the boundary layer, it seems that the average values of both components of the fluid velocity are very close to the desired ones (the values predicted during the preliminary design).

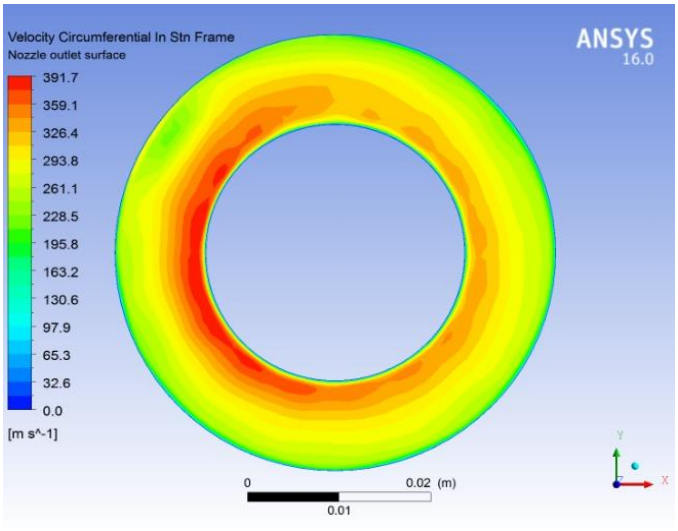

Figure 16. Contour of circumferential velocity at nozzle outlet

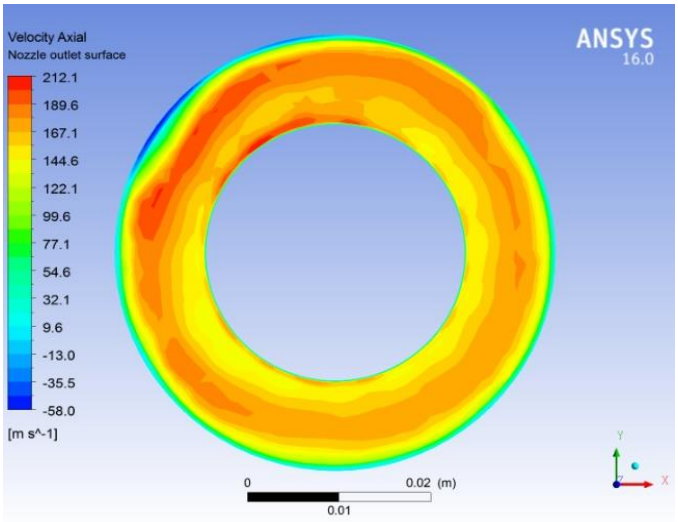

Figure 17. Contour of axial velocity at nozzle outlet

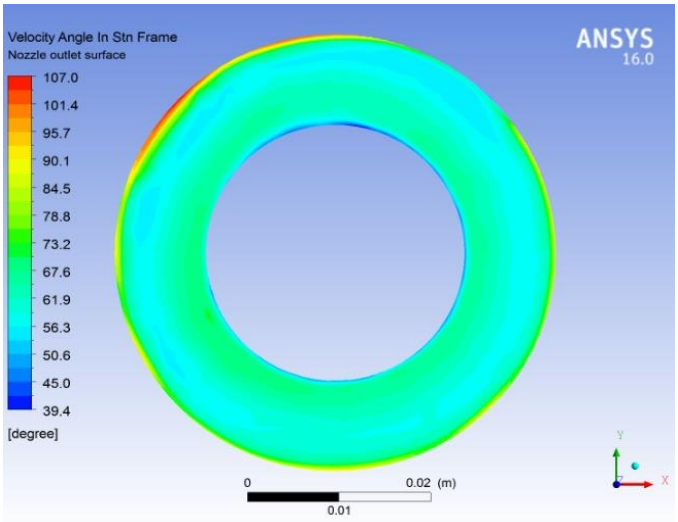

Figure 18. Contour of velocity angle at nozzle outlet

Therefore, the performed analysis has demonstrated that the geometry of the nozzle and of the volute calculated in the preliminary design chapter respects the objective of the project and can be coupled with the rotor obtaining the desired performance.

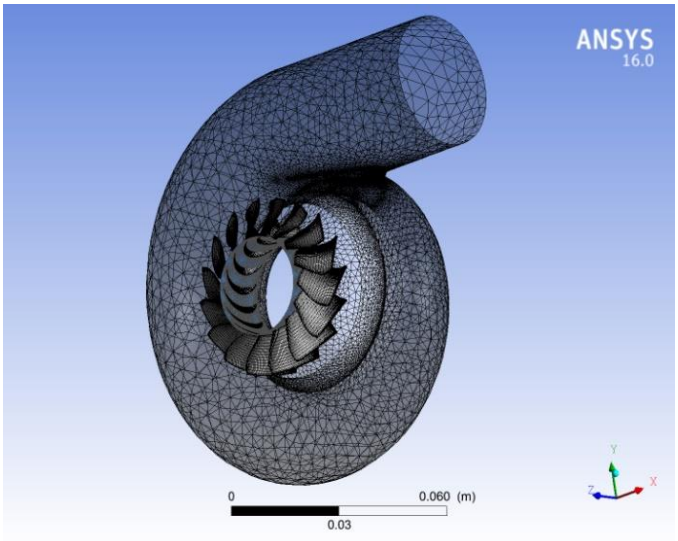

Figure 19. Mesh of the whole turbine. isometric view

CFD simulation of the whole turbine

As shown in the previous paragraph, the thermo-fluid-dynamic conditions at the inlet section of the rotor change point by point and this non-constancy of physics quantities adversely effects the performance of the turbine. So, it is necessary to simulate the entire machine (volute + nozzle + rotor) in order to investigate the behavior of the fluid within the turbine [11]. Therefore, the mesh of both the complete rotor and the fixed part of the machine (volute and nozzle) have been imported into the solver, interfaced and simulated. For solving this turbomachinery problem involving a fixed domain and a rotating one using CFD, there exists specific and special models to be applied, and one of the models is the Moving Reference Frame (MRF). In MRF model, a moving reference frame permits an unsteady problem (with respect to the absolute reference frame) to become steady in respect to the moving reference frame. In other words, it is a steady state approximation where the fluid zone in the fan region is modelled as a rotating frame of reference and the fixed zones are modelled in a stationary frame [12], [13], [14]. The behavior of the fluid has been again modified setting a c_p variable with the temperature according to a 8th degree polynomial.

Table 3 resumes the boundary conditions chosen for the simulation.

Table 3. Inlet and outlet boundary conditions

Pressure Inlet	
Total Pressure	235360 [Pa]
Total Temperature	1097.34 [K]
Direction Specification	Normal to bound
Pressure Outlet	
Static Pressure	145750 [Pa]
Backflow Tot. Temp.	990 [K]
Backflow Direction Spec.	Normal to bound

The turbulence model employed is one of the most commonly used for turbomachinery CFD simulation, the k-ω model [15], [16]. It is a two equations model, that means, it includes two extra transport equations to represent the turbulent properties of the flow. This requires specifying two more boundary conditions for the two new equations. As performance method for the turbulent boundary conditions setting, it has been chosen the "Intensity and Viscosity Ratio" method; details in Table 4.

Table 4. Turbulent boundary conditions

Inlet	
Turbulent Intensity	5%
Turbulent Viscosity Ratio	10
Outlet	
Backflow Turbulent Intensity	5%
Backflow Turbulent Viscosity Ratio	10

About the convergence criteria, each calculation of this project is judged completed only when the residuals reach values < 1e-5 (in terms of RMS) and when the monitored quantities (outlet total pressure, outlet Mach number and outlet mass flow) remain stable during the calculation.

Mesh sensitivity analysis

The selection of the most appropriate number of elements must come from a compromise between the accuracy of the results and computational time. The mesh sensitivity analysis has the objective to analyze how one or more monitored quantities evolve increasing the number of elements of the mesh. When a certain number of elements is reached, the monitored quantities do not change appreciably by increasing again the number of elements; at that point using a higher number of cells would not lead to more accurate simulation results while the calculation would require a longer computational time and the results would not be more accurate. The results of the analysis are provided in the following tab and plots:

Table 5. Mesh sensitivity analysis results

Number of cells					
Case #	**Stator (*10^3)**	**1 rotor passage (*10^3)**	**Total (*10^3)**		
1	50	10	210		
2	200	20	520		
3	400	60	1360		
4	500	80	1780		
5	600	100	2200		
6	800	160	3360		
7	1000	200	4200		
CFD results					
Case #	**η_{T-S} [-]**	**Mex [-]**	**Tot Pres. ex [Pa]**	**Mass Flow [kg/s]**	**Computational time [h]**
1	0.697	0.316	156322	0.1144	1
2	0.704	0.322	156639	0.1158	4
3	0.701	0.327	157030	0.1154	8
4	0.700	0.328	157128	0.1152	12
5	0.699	0.329	157137	0.1151	15
6	0.698	0.330	157182	0.1151	23
7	0.698	0.331	157233	0.1151	32

Looking at the progression of mass flow, efficiency and Mach number with the number of grid elements, the variation becomes less significant from Case 3 on. At the same time, the computational time

begins to be noticeable from Case 3 as well; therefore, it has been decided to opt for the number of elements of Case 3 as declared before in this paper.

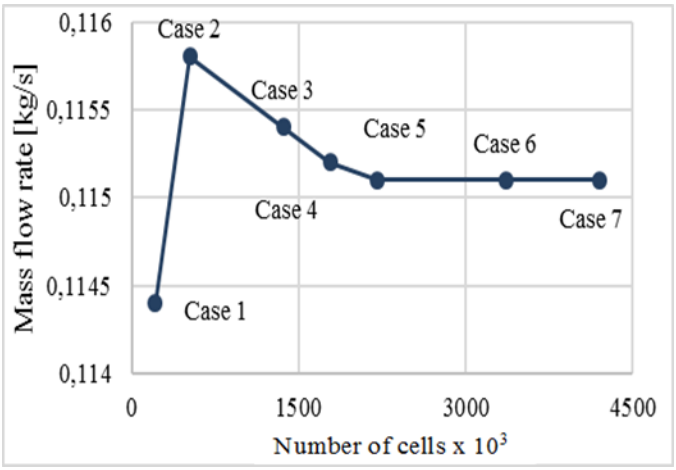

Figure 20. Mass flow rate vs. Cells number

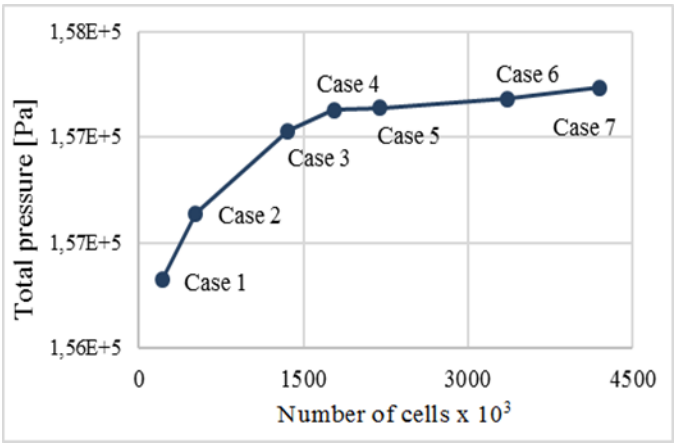

Figure 21. Total pressure at rotor outlet vs. Cells number

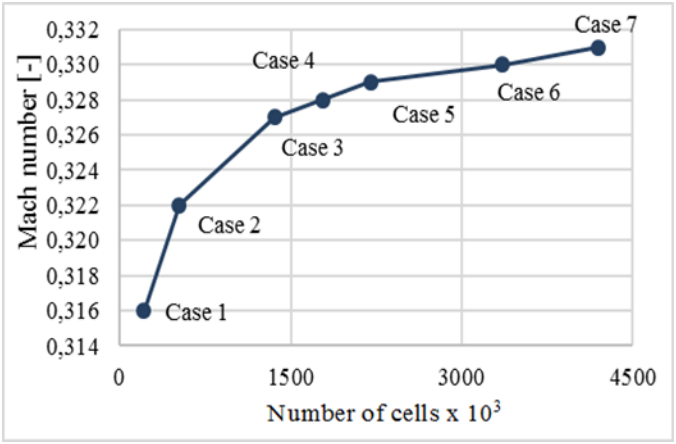

Figure 22. Mach number at rotor outlet vs. Cells number

Results of the complete turbine analysis

It must be reminded that the geometry, whose results are shown in this paragraph, comes from an iterative process of modification and selection of the most efficient geometry. Table 6 resumes all the principal parameters that characterize the performance of the new axial turbine:

Table 6.: CFD results

Parameter	**Unit**	**Span 0.15**	**Span 0.50**	**Span 0.90**
SWC, ψ	[-]	2.65	1.82	1.34
SFC, φ	[-]	0.88	0.66	0.46
Reaction degree, R	[-]	0.35	0.58	0.76
Outlet Absolute velocity	[m/s]	224.3	212.1	168.9
Outlet Circ.tial velocity	[m/s]	58.3	50.1	5.6
Outlet Axial velocity	[m/s]	216.6	206.1	168.8
Outlet Flow angle	[°]	15.1	13.7	1.9
Outlet Relative velocity	[m/s]	376.2	395.3	387.1
Outlet Circ. relative velocity	[m/s]	306.8	339.4	350.9
Outlet Relative angle	[°]	54.7	59.2	65.1
Max. Mach number	[-]	0.67	0.77	0.81
Outlet Abs. Mach number	[-]	0.36	0.35	0.28
Outlet Rel. Mach number	[-]	0.61	0.64	0.63

The table reports three values for each parameter, calculated at 15%, 50% and 90% of span respectively. The first three parameters are dimensionless quantity, like stage work coefficient, stage flow coefficient and degree of reaction [17]. They have been calculated with the following relationships:

$$\psi = 2\frac{W_{\theta 2} - W_{\theta 3}}{U} \quad (72) \qquad \phi = \frac{C_{x3}}{U} \quad (13)$$

$$R = \frac{(W_3^2 - W_2^2)/2}{U(C_{\theta 2} - C_{\theta 3})} \quad (14)$$

Where the subscript “2” indicates the parameters relative to the rotor inlet section and the subscript “3” indicates the ones relative to the rotor outlet section,

Figure 23 shows the relative Mach number contour at span 0.5; in particular, the maximum value of this parameter has been calculated at three different height of the blade and it never reaches excessive values, the maximum is 0.81 at 90% of span, so the flow is always subsonic. Figure 24, instead, shows the contour of static pressure at the same blade height. In that picture, it is easier to notice that the flow condition differs from blade to blade.

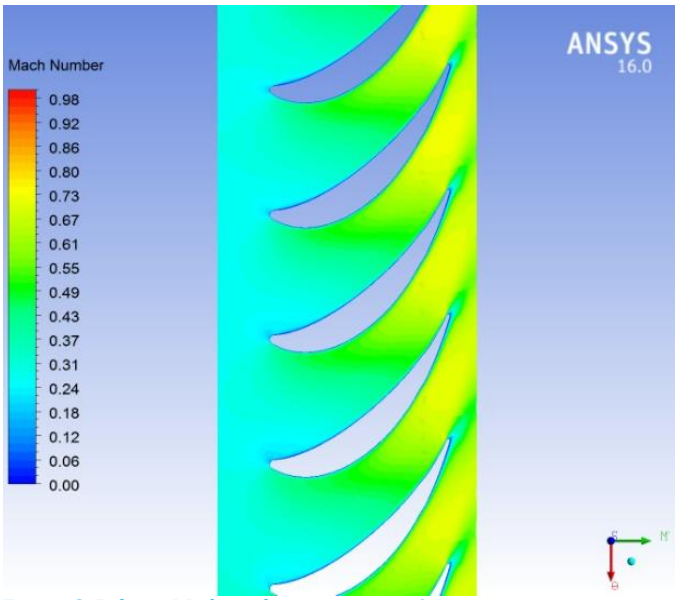

Figure 23. Relative Mach number contour, span 0.5

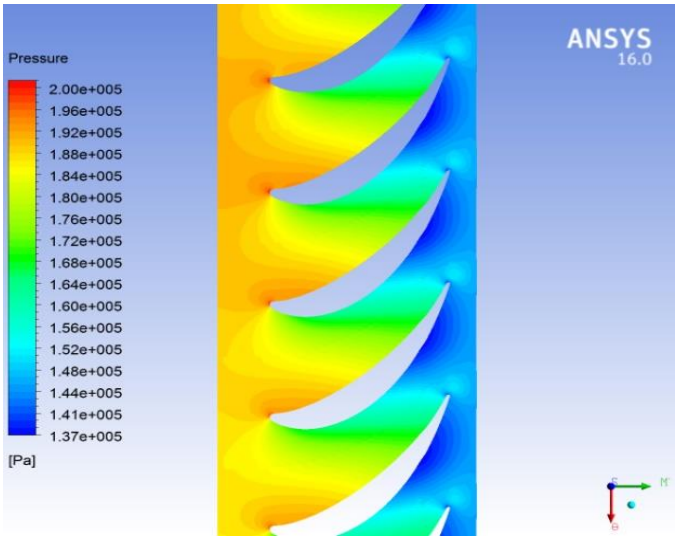

Figure 24. Static pressure contour, span 0.5

It is useful to underline that the conditions at the exit of the nozzle obviously effect the condition of the fluid within the rotor; so, every blade works in a slightly different condition. All the velocity values, the Mach numbers, the forces acting on the blades (as well as the quantities showed in Table 6), are averaged values.

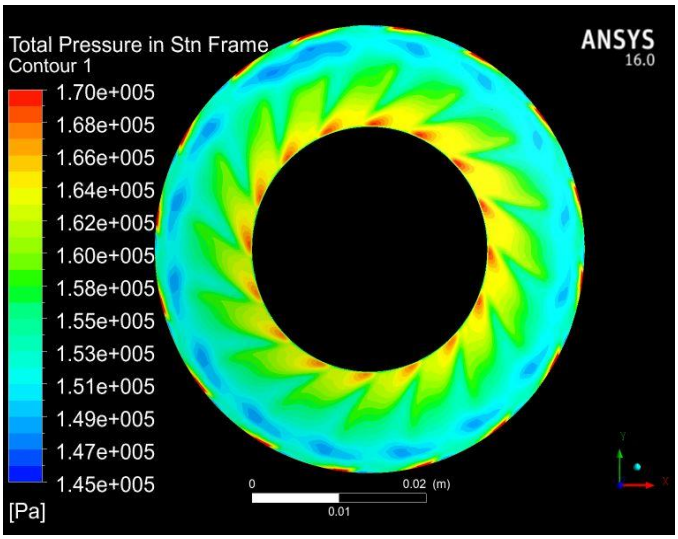

Figure 25. Total pressure contour

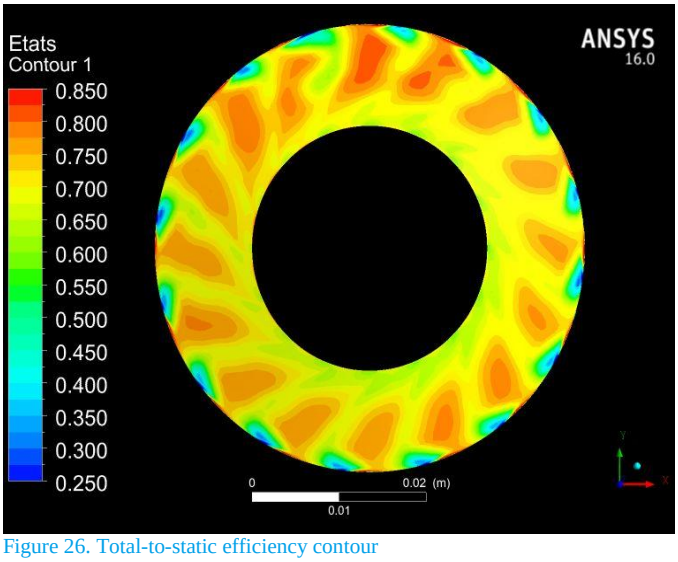

Figure 26. Total-to-static efficiency contour

In order to better visualize the non-uniformity of the flow conditions and its effect, Figure 25 represents the contour of total pressure calculated on the rotor outlet surface. The non-uniformity of the thermodynamic conditions translates into non-uniformity of performance; indeed, Figure 26 demonstrates that the turbine total-to-static efficiency is not a uniform value on rotor outlet surface [18].

Therefore, it is clear that also the calculated performance of the machine is an averaged value like presented in Table 7.

Table 7. Turbine performance compared to AxStream results

Results	Power [W]	Mass Flow [kg/s]	η_{T-S}	η_{T-T}
Final Turbine	11340	0.115	70.00%	82.40%
AxStream	12397	0.113	77.00%	86.00%

Off-design analysis

Building a performance map of the turbine is the best way to characterize the behavior of the machine and would represent the goal of a turbomachinery design process. The map synthetizes the performance of the turbine and allows to couple it with the stock compressor in a 1D model to evaluate the benefits on the engine performance. The performance of the new axial turbine has been obtained carrying out many CFD simulations changing the boundary conditions to reproduce the same procedure followed during map measurement. Leaving the rotational speed, the inlet total temperature and the outlet static pressure unvaried, and changing case-by-case the inlet total pressure, several points of a constant-speed line have been obtained. Then, repeating the same process for different values of the rotational speed, has been obtained.

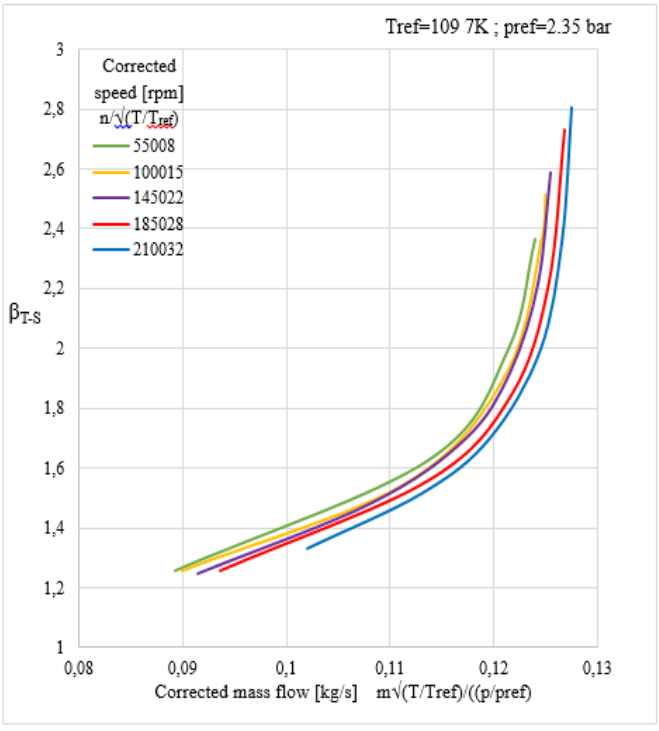

Figure 27. New axial turbine performance map

Figure 27 displays the performance map of the new axial turbine in the most common form, total-to-static expansion ratio vs. corrected mass flow at different rotational speed. The map reports the reference pressure and temperature as well, they have been used to correct mass flow rate and speed, like in a typical turbocharger turbine map; the

slope of each constant-speed lines increases with the pressure ratio but at certain point they became vertical due to the chocking of the flow within the rotor channels. So, it is possible to identify a very narrow range of chocking corrected mass flow that is around the value of 0.125 kg/s.

Calculation of the modified turbocharger matched with the engine

Once the performance map of the axial turbine is obtained, it possible to use the 1D engine model employed in the first part of this work to virtually test the new configuration. Replacing the original GT1548 turbine with a completely new one leads to a different matching between the engine and the turbocharger. The new axial machine is going to work with different mass flow rate, different inlet pressure and efficiency to ensure the same target boost pressure at the compressor outlet. Obviously, the turbine speed and the delivered power will be different, thus, the compressor operating condition will be different, too. At the same time, the engine performance could be different with the new turbine, in fact the different wastegate valve opening and back-pressure caused by the new turbine will affect the PMEP of the engine. It is clear that even if the axial turbine performance seems to be better than the original one at design point, the new engine-turbo matching could deliver negative results. Therefore, a simulation of the new system engine-turbocharger is essential to evaluate if the new turbine is actually suitable for replacing the original one without reduce the engine performance.

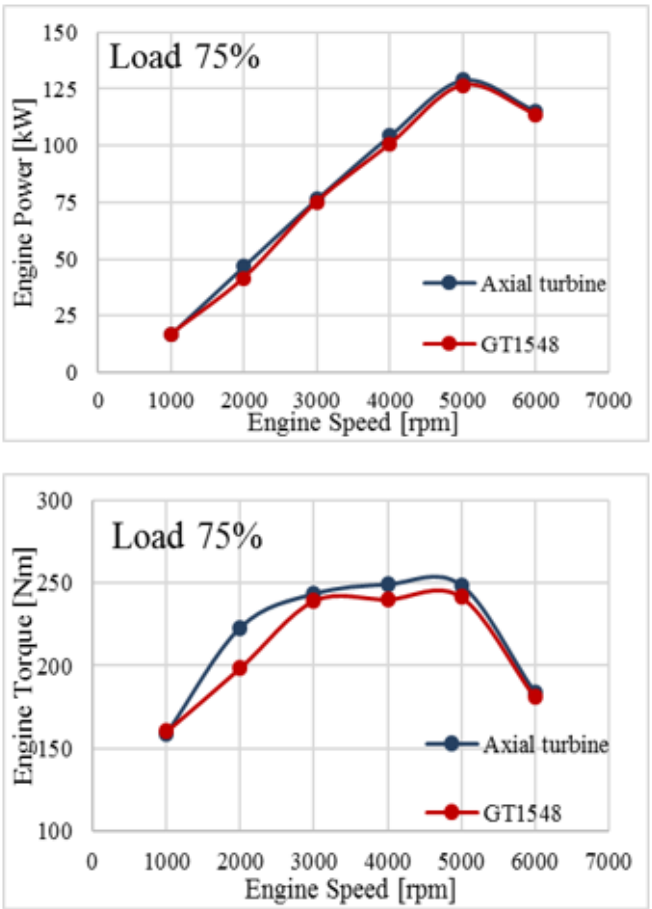

Figure 28. Comparison between the axial turbine and the original one in terms of engine power and torque

So, the new turbine map has been imported into the 1D engine model and a simulation has been run. During this new simulation, the target boost pressure has been left unchanged respect to the initial model so that it is easier to isolate the effects of the new map on the system.

Before showing the results of the simulation, it is worth to highlight that the results of the new configuration can be further improved by re-calibrating the engine.

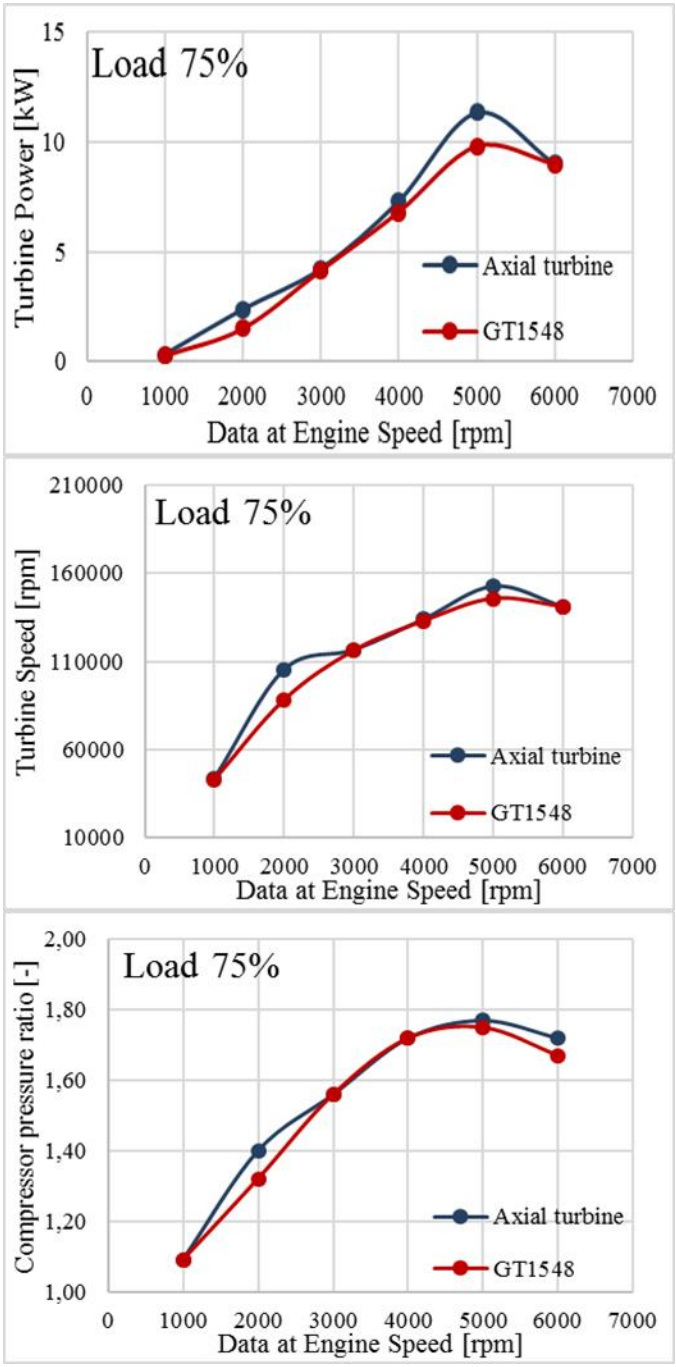

Figure 29. Comparison between the axial turbine and the original one in terms of power, rotational speed and compressor pressure ratio

Figure 28 illustrates the comparison between the power curves and torque curves of the engine boosted by the two configurations of turbocharger at 75% of engine load. The power curves of the of the two configurations are very close to each other while some difference exists on the torque curves. In fact, the engine equipped with the axial turbine is able to deliver the maximum torque (or values close to the maximum toque, flat curve trend) for a wide range of rpm (2500 - 5000), therefore, the performance of this new configuration is higher than the stock one at every rpm; that could be considered a positive result.

Finally, the set of diagrams in Figure 29 compare the performance of the two turbocharger configurations. The power of the axial turbine is higher than the GT1548 power at each engine speed and it reaches higher for engine speed of 2000 and 5000 rpm that are the operating conditions where the power and the torque of the engine exceed the most the old configuration. At the same time, the new turbine allows the compressor to generate a pressure ratio very close to the original configuration except for some (2000 and 5000 rpm of engine speed) point where a slightly higher boost pressure is achieved.

The variable geometry – vaneless concept

This section aims to discuss some preliminary results that have obtained by applying the variable geometry concept to the vaneless axial flow turbine.

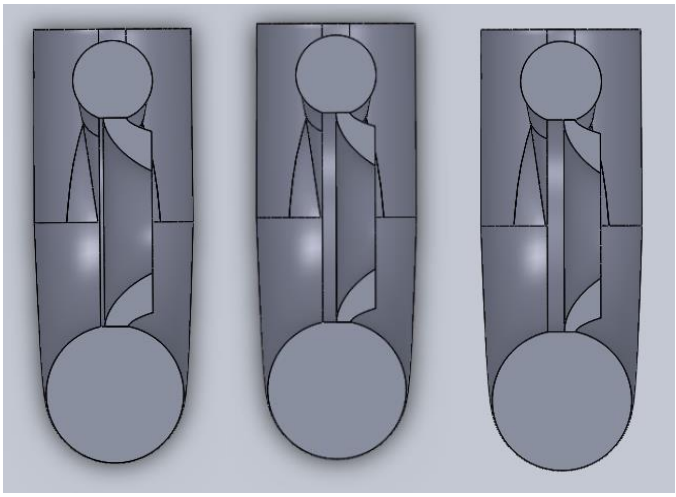

Figure 30. The variable inlet area nozzle (left to right: full opening to closing)

Such a concept founds on the possibility of axially shifting the radial flow nozzle with respect to the volute. A nozzle right-shift results in a reduction of the interface area between volute discharge and nozzle inlet (Figure 30) so decreasing the flow capacity of the volute – nozzle system. This solution appears to be less challenging by the point of view of mechanical and thermal stresses if compared with the classical variable geometry vaned stators and the final results demonstrate its effectiveness.

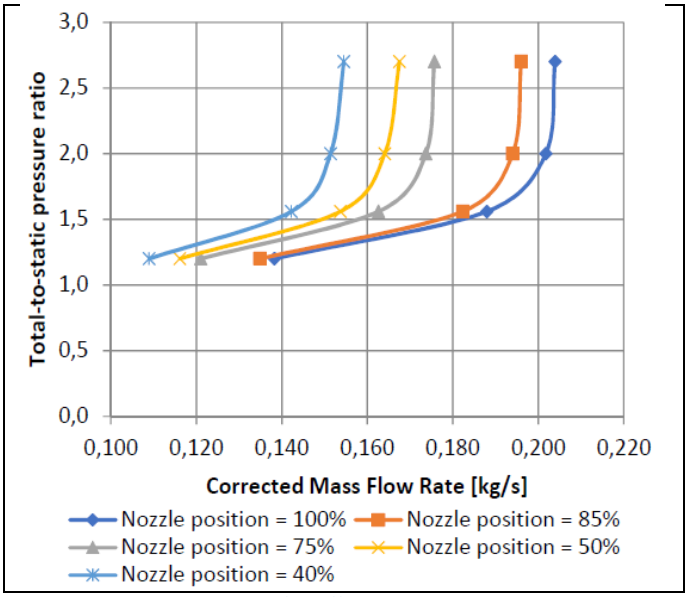

Figure 31 Turbine operating lines for different nozzle openings.

As a matter of fact, Figure 31 shows that the variable nozzle opening allows a turbine operation in a wide range of exhaust flow rates, while keeping the same level of pressure ratio. The results in Figure 31 have been obtained for a given corrected speed (150000 rpm) but they represent a part of a full off-design analysis of the variable geometry vaneless turbine.

If looking at some details of the rotor flow field (Figure 32), it can be observed that the reduction in the nozzle inlet area induces a decrease in velocity and Mach number levels through the moving blades, so allowing the turbine to adapt to changes in the mass flow rate range [19].

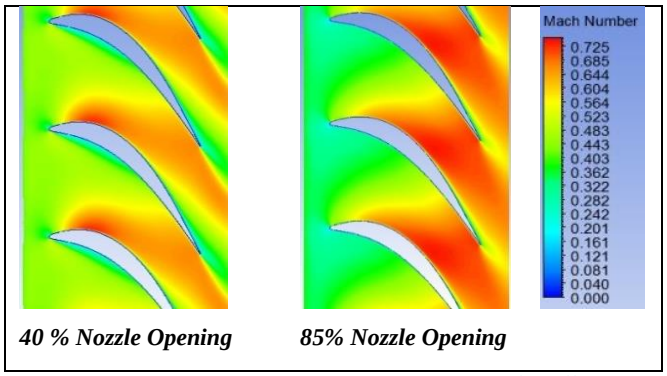

Figure 32. Relative Mach number contours at rotor mid-span for different nozzle openings

Once obtained the complete turbine performance map, the 1D simulation of the engine – turbocharger matching leads to definition of the engine torque curves for different nozzle openings (Figure 33) [20]. This figure gives evidence of a high sensitivity of the engine performance in the (100% - 85%) range of nozzle opening. Conversely, a weaker sensitivity can be observed for further reductions of the nozzle area.

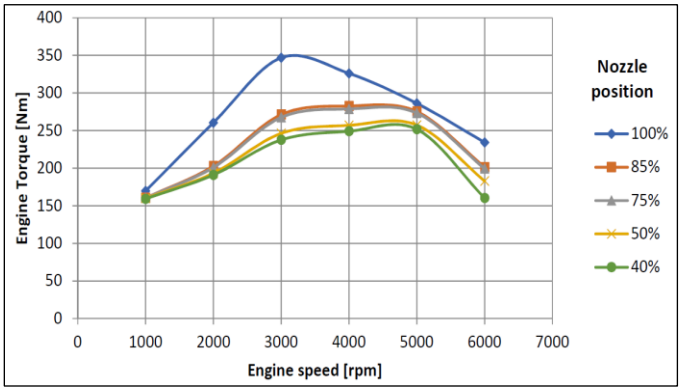

Figure 33. The VNT effect on the engine torque (at WOT)

This demonstrates that such a preliminary application of the variable nozzle concept is worthy of an accurate refinement, in order to ensure a more continuous response of the engine performance to changes in inlet nozzle area. On the other hand, the potential of this solution can be already put into evidence. Actually, while the intake throttle opening exerts the air flow control by means of a total pressure loss, the nozzle variable geometry introduces a second degree of freedom. In other words, changes in air flow rate levels are now possible also by acting directly on the turbine – compressor matching. This way should be conceptually more efficient, provided that the variable area system does not induce additional pressure losses.
Basing on the above statement, charts like the one in Figure 34 indicate that the double degree of freedom allows, for example, the selection of the combination (nozzle – throttle opening) that leads to minimum fuel consumption for a given engine torque. Similarly, the effect of these

parameters on the in-cylinder pressure peaks and, consequently, on the knock inception may be examined.

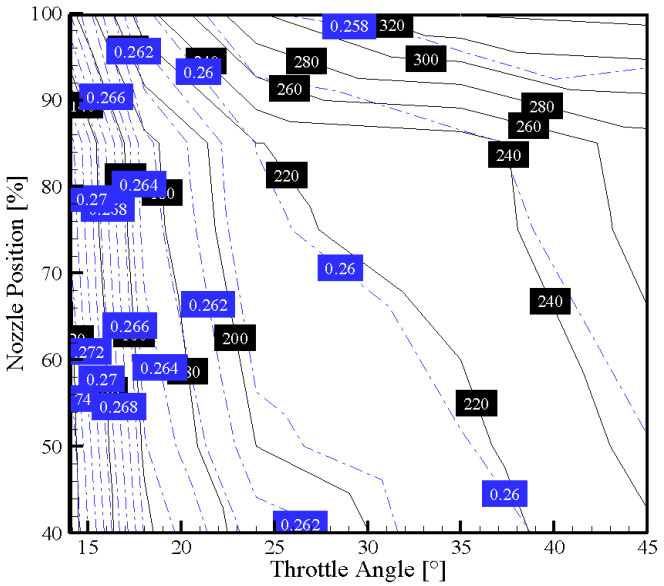

Figure 34. Engine torque and fuel consumption contours at 3000 rpm. Solid black line: engine torque; Dash-dot blue line: BSFC

As a first example of the possible optimizing strategy, Figure 35 shows the engine curve that is obtainable by selecting the most proper values of nozzle openings. through the identification of the most suitable points on each curve of the previous Figure 33. In this case, the objective is obtaining a much flatter curve and this represents a noticeable improvement with respect to the employment of the original radial flow turbine.

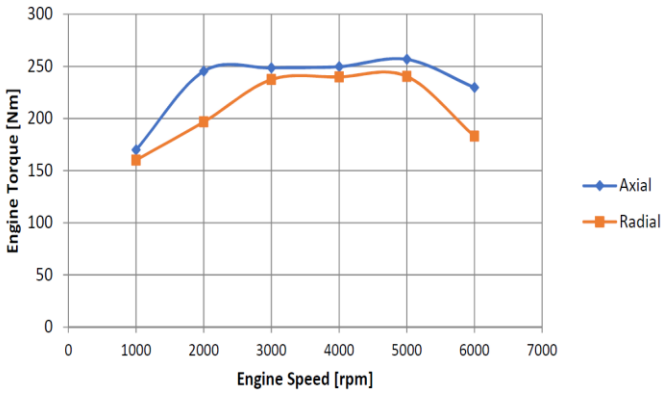

Figure 35 Comparison of engine torque curve with radial flow and variable nozzle axial flow turbine at WOT.

Conclusions and future developments

The simulation of the system engine-modified turbocharger produced very interesting results. The new axial turbine is able to provide the compressor with a proper amount of power so ensuring, in each operating condition, an adequate boost level of the engine. In fact, the modified turbocharger produces the same performance of the original one in terms of engine power and torque and, in some cases, even higher. Moreover, the most impressive improvement concerns the efficiency of the turbine; the new design operates very efficiently in all the simulated conditions. This is an important result since the stock Garrett turbine has been replaced by a machine equivalent in terms of engine performance in steady state conditions. Furthermore, using an axial turbine, which has intrinsically a lower inertia compared to the radial one, as proved by the Ford and Honeywell researches, the turbo-lag phenomenon will be reduced.

This project has produced a fluid-dynamic design that could be further improved. Some interesting CFD investigations can be carried out in transient condition and under pulsating flows. A structural analysis could provide more information about the reliability of the machine.

In the final part of this work, the initial design has been considered as with a variable geometry mechanism able to vary the cross-sectional area of the nozzle thanks to a sliding hub wall. A better acceleration of the fluid even at low mass flow rates is allowed and a faster acceleration of the turbocharger is expected (further improvement of the turbo-lag). The first examples of engine – VNT matching have demonstrated that flatter engine torque curves may be obtained and a more efficient engine management is achievable in a wide range of loads and rotational regimes.

Finally, future work will be addressed to the identification of the optimal solutions for the variable nozzle turbine. The machine manufacturing and testing will verify if the axial solution introduces real benefits in terms of transient response of the turbocharger.

References

1. Association ACEA - European Automobile, «Passenger Cars» [Online]. Available: http://www.acea.be/automobile-industry/passenger-cars.
2. Market and Markets, 2014, "Turbocharger Market by Vehicle Types (Passenger and Commercial), Fuel Types (Diesel and Gasoline) and Geography - Global Trends and Forecasts to 2017".
3. Bauer, Dipl.- Ing. K-H.; C. Balis, M.S.E., G. Donk, «The Next Generation of Gasoline Turbo Technology» in Internationales Wiener Motorensymposium, 2012.
4. Baskharone, 2006, Principles of Turbomachinery in Air-Breathing Engines, Cambridge, ISBN-10 0-521-85810-0.
5. Rahnke C.J., and Company F. M.,1988 , "Axial Flow Automotive Turbochargers" ASME 85-GT-123.
6. Cox H., and Craig H.,1970, "Performance Estimation Of Axial Flow Turbines" Instn Mech Engres, Vol 185 32/71, pp. 407-424.
7. SoftIn Way Incorporated, AxStream.
8. N. Watson, M.S. Janota, Turbocharging the Internal Combustion Engine, London and Basingstoke: The Mecmillan Press LTD, 1982, ISBN: 0 333 24290 4.
9. Hakeem I., Costall A., Su C., and Martinez-Botas A.,2007, "Effect of volute geometry on the steady and unsteady performance on mixed flow turbines" in Proceedings of the Institution of Mechanical Engineers Part A Journal of Power and Energy 221(4):535-549 June 2007, doi:10.1234/09576509JPE314.
10. C. Xu, R. Amano, 2006, "Eliminating static pressure distortion" Paper No. GT2006–90001.
11. Ramezani A., Remaki L., Blanco J., and Antolin J.,2014, "Efficient Rotating Frame Simulation in Turbomachinery" ASME paper GT2014-25101.
12. LearnCAx , "CFD Modeling for Turbomachinery using MRF Model".
13. Schoenenborn H., and Ashcroft G., 2014, "Comparison of Non-Linear and Linearized CFD Analysis of the Stator-Rotor Interaction of a Compressor Stage", ASME paper GT2014-25256.
14. Casartielli E., Mangani L., Hanimann L., Mokulys H., and Mauri S., 2013, "Development of a Novel Mixing Plane Interface Using a Fully Implicit Averaging for Stage Analysis", ASME paper GT2013-94390.
15. George A. St., Driscoll R., Gutmark E., Munday D., 2014, "Experimental comparison of axial turbine performance under steady and pulsating flows", ASME paper GT2014-27110.

16. Du P., Ning F., 2013, "Simulating periodic unsteady flows using cubic-spline based time collocation method", ASME paper GT2013-94195.
17. Roclawski H., Gugau M., Langecker F., and Bohle M., 2014, "Influence of Degree of Reaction on Turbine Performance for Pulsating Flow Conditions" ASME paper GT2014 - 25829.
18. Feng Z.,Li J., and Sun,2009, "Effects of Tip Clearance on Unsteady Flow Characteristics in an Axial Turbine Stage",ASME paper GT2009-59828.
19. Chen L., Zhuge W., Zhang Y., Xie L.,Zhang S., 2011, "Effects of pulstation flow conditions on mixed flow turbine performance", ASME paper GT2011-451*4.
20. Gugau M., Roclawski H., 2012, "On the design and matching of a turbocharger turbine for pass car gasoline engines", ASME paper GT2012-68575.

Nomenclature

A	Cross Section Area [m^2]
C	Velocity [m/s]
C_θ	Tangential Velocity [m/s]
C_r	Radial Velocity [m/s]
C_x	Axial Velocity [m/s]
Co	Isentropic Speed [m/s]
c_p	Specific Heat [kJ/kg/K]
Dm	Mean Diameter [m]
Ds	Specific Diameter [-]
$\Delta h_{t,id}$	Ideal Total Enthalpy Drop [J/kg]
$\Delta h_{ts,id}$	Ideal Total to Static Enthalpy Drop [J/kg]
M	Mach Number [-]
$\dot{m}$	Mass Flow Rate [kg/s]
n	Rotational Speed [rpm]
Ns	Specific Speed [-]
r	Radius [m]
R	Universal Gas Constant [kJ/kgK]
T	Static Temperature [K]
T_t	Total Temperature [K]
U	Blade Speed [m/s]
W	Relative Velocity [m/s]
W_x	Relative Axial Velocity [m/s]
W_θ	Relative Tangential Velocity [m/s]
W_r	Relative Radial Velocity [m/s]

Greek characters

γ	Specific Heat Ratio [-]
ρ	Static Density [kg/m^3]
ρ_t	Total Density [kg/m^3]
ω	Angular velocity [rad/s]
ψ	Azimuth Angle [rad]
η_{T-S}	Total-to-Static Efficiency
η_{T-T}	Total-to-Total Efficiency

Abbreviations

CFD	Computational Fluid-Dynamic
MRF	Moving Reference Frame
$PMEP$	Pumping Mean Effective Pressure
RMS	Root Mean Square
VNT	Variable Nozzle Turbine